Scientia Iranica D (2019) 26(6), 3656–3671

Sharif University of Technology
Scientia Iranica
Transactions D: Computer Science & Engineering and Electrical Engineering
http://scientiairanica.sharif.edu

A new computing perturb-and-observe-type algorithm for MPPT in solar photovoltaic systems and evaluation of its performance against other variants by experimental validation

V. Bhan[a,1], A.A. Hashmani[a], and M.M. Shaikh[b,c,*]

a. *Department of Electrical Engineering, Mehran University of Engineering and Technology, Jamshoro, Pakistan.*
b. *Department of Basic Sciences and Related Studies, Mehran University of Engineering and Technology, Jamshoro, Pakistan.*
c. *Supply Chain and Operations Management Research Group, Mehran University of Engineering and Technology, Jamshoro, Pakistan.*

Received 5 August 2019; accepted 8 September 2019

KEYWORDS
Maximum power point tracking;
Perturb-observe algorithm;
Solar photovoltaic;
Irradiance;
Stability;
Oscillations;
Tracking speed.

Abstract. Solar energy is becoming the mainstream energy source by drawing considerable attention of analysts these days. The output power of a photovoltaic (PV) system fluctuates with temperature and sunlight, affecting its efficiency. To extract accessible power by a PV system, Maximum Power Point Tracking (MPPT) method is adopted. A famous strategy regularly utilized due to its simplicity and low cost is the Perturb and Observe (PO) algorithm. However, there are a few downsides with PO algorithm, which result in power loss and low efficiency. We compared the performance of the conventional PO with some enhancements, especially a recent PO variant, for MPPT. Experiments were conducted at different irradiances and temperature levels in two ways, namely with load and with battery, by conventional PO and its variants. The strategy to reach optima and stability of the methods were discussed. The PO variants were rated from the viewpoints of stability, accuracy, post-MPP oscillations, and tracking speed. The modifications were proven to be fruitful for the practitioners working with MPPT in PV solar systems using PO algorithms. Simulation results were validated using real-time experimental results. The new PO variant appeared to be a reliable computing algorithm for MPPT in solar PV systems.

1. Introduction

Renewable sources of power are gaining increasing significance against the enormous utilization and fatigue of petroleum derivatives. Among a few sustainable power sources, photovoltaic arrays have numerous applications, e.g., pumping of water, charging of batteries, hybrid systems for vehicles, and PV systems connected by grids [1]. A PV system is most generally categorized as a stand-alone PV, grid-connection, or hybrid system.

The operating conditions usually affect the performance of stand-alone PV systems. These systems are mainly utilized in places much away from a conventional power generation system. Awan et al. [2] noted that ambient cell temperature, load profile, and the influence of insolation of PV generators on a

1. *Present address: Department of Electrical Engineering, Institute of Business Administration University, Sukkur, Pakistan.*
*. *Corresponding author. Tel.: +92 333 2617602*
E-mail addresses: veer.bhan@iba-suk.edu.pk (V. Bhan); ashfaquehashmani1@gmail.com (A.A. Hashmani); mujtaba.shaikh@faculty.muet.edu.pk (M.M. Shaikh)

doi: 10.24200/sci.2019.54183.3635

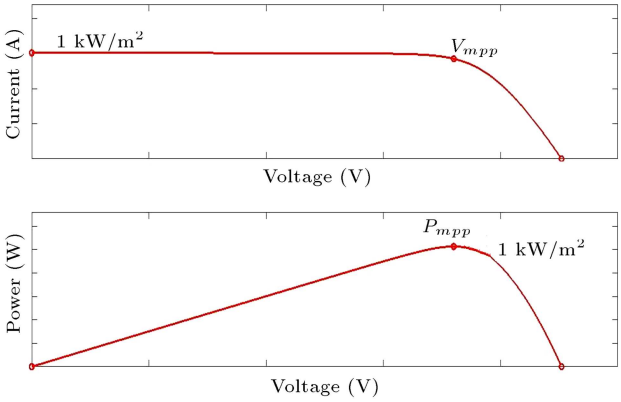

Figure 1. $I-V$ and $P-V$ characteristics of a solar photovoltaic panel.

particular cell efficiency would affect the amount of maximum power extracted. Extraction of the highest amount of power is important to make an efficient PV system. To this aim, Maximum Power Point (MPP) trackers are utilized to achieve the best operation of PV systems. Figure 1 represents general $I-V$ and $P-V$ characteristics for a solar photovoltaic panel, where V_{mpp} and P_{mpp} are the voltage and power characteristics of the MPP at an irradiance of 1 W/m^2. The general block diagram of a stand-alone PV system with MPP tracker is shown in Figure 2. As discussed by Putri et al. [3] and Babaa et al. [4], inefficiencies of the solar panels, mostly below 25%, have been a very serious issue in solar power systems since the advent of MPPT algorithms in 1980s. MPPT methods attempt to minimize the inefficiencies by solar modules and enable efficient and reasonable extraction of solar power.

Unlike mechanical trackers, the MPP trackers comprise some components involving charge controllers, micro-inverters, and string inverters [3,4]. Microprocessors in MPPT systems are used to examine electrical input, like current and voltage, and follow a defined method to make necessary corrections for maintaining the MPPs. Up to now, a number of circuits and methods for the development of MPP trackers have been presented. After the development of MPPT algorithms for the first time, many successful enhancements have been made in the literature [3,4] by incremental conductance, steady voltage strategy, consistent current technique, cut-off technique, Perturb and Observe (PO) technique, and Open Circuit (OC) voltage strategy. Among the abovementioned enhancements, PO is the mostly utilized one since it is a basic and simple-to-perform method. The performances of Hill Climbing (HC), Incremental Conductance (INC), and Fuzzy Logic (FL) controller techniques were compared with that of the PO method by Rezk and Eltamaly [5]. By applying some changes to the FL part in MPPT algorithms, a hybrid MPPT method was proposed by Bahrami et al. [6] through blending two existing algorithms. It was demonstrated that the new hybrid algorithm was efficient under rapidly changing environmental and transient conditions. By combining the HC and a variant of Particle Swam (PS) optimization algorithm, a new and computationally efficient MPPT method was suggested by Chaieb and Sakly [7] for partially shaded cases.

The calculations in the conventional PO algorithm have a few disadvantages as highlighted by Rezk and Eltamaly [5]. For example, under fast changing climate conditions, the algorithm has low tracking speed and the PV system oscillates when operating around MPP, as discussed by Salas et al. [8].

The modified PO MPPT control method is another technique that, unlike the PV system in the typical PO strategy, controls voltage and current by directly managing the duty cycle of the DC to DC

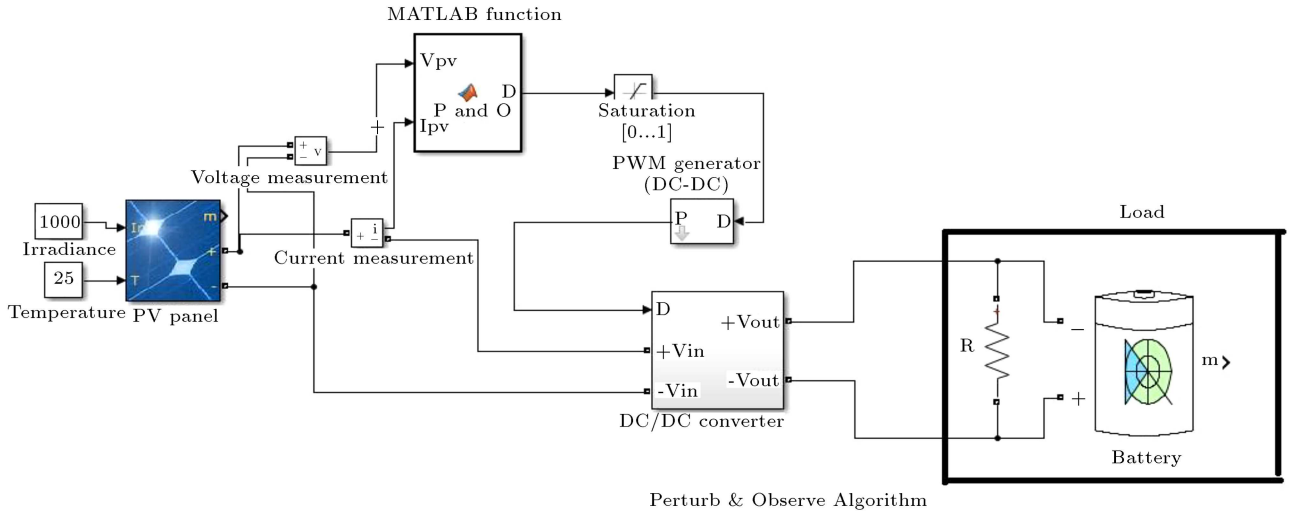

Figure 2. General block diagram of a stand-alone PV system with MPPT.

buck converter. Simplicity and high tracking speed are benefits of the modified PO MPPT algorithm presented by Thenkani and Kumar [9].

In fast changing climate conditions, PO calculation may sometimes take the system far away from the MPP [10-14]. The variable advance size procedure utilized as a part of PO calculation has a quicker reaction in following the MPP. However, there still remains the fundamental issue of oscillations of the operating point around the MPP. In PO calculation, only a single variable's incentive out of two–voltage and current–is used and continued by observing the results. This issue arises because the tracker cannot perceive whether the adjustment in control is because of perturbation or due to change in climate condition (irradiance or temperature). Therefore, the operating point is constantly in the oscillatory state. PO calculation is generally modified by utilizing the "lessening and fix" technique to tackle this issue. This technique uses estimates of both variables (current and voltage) to inform the tracker that whether perturbation or change in climate conditions (irradiance or temperature) enforces the adjustment in control. The variable advance size method has been utilized to replace the "reduction and fix" system [1].

Researchers have proposed enhanced variants of the conventional PO algorithm to accelerate tracking speed and increase efficiency under different atmospheric conditions, including various temperature and irradiance [7,10-12,15]. The improvement of charge rate using PV MPPT in ultracapacitor and battery was measured by Rajani and Pandya [16]. They also investigated the payback with improvement in efficiency and charging rate. In addition, some recent studies have applied MPPT techniques to different PV systems by incorporating various controllers. Some examples are the predictive control design of marine PV systems by Tang et al. [17], the new temperature controller with incremental conductance for indoor PV systems offered by Shahid et al. [18], the backstepping nonlinear controller with asymptotic stability for PV systems presented by Arsalan et al. [19], and advanced MPPT control design of PV-solar pumps by El-Khatib et al. [20].

In this paper, the performances of a new PO variant and some PO-based MPPT algorithms in the photovoltaic solar systems are investigated for load and battery. The methodology, algorithms, implementation, and analysis of the results for the conventional PO and its variants will be presented in detail. Finally, on the basis of stability against maximum power, post MPP oscillations, and tracking speed, the methods will be rated for the load and battery cases. The recommendations provided in this study will help practitioners and researchers to select reliable PO-based MPPT algorithms for solar photovoltaic applications.

After introducing the topic, its importance, the relevant literature, and the main objectives of the study in this section, the remainder of the paper is organized as follows. Section 2 is devoted to introducing and comparing the algorithms of the conventional PO method and some of its enhancements. Also, the flowcharts of the enhancement methods are presented in this section. Section 3 explains the incorporated setup for numerical simulations, test conditions, and the applications of the PO variants in the battery and load cases. In addition, the results are presented and discussed, and some recommendations are given based on the comparison in this section. The section on conclusion is the final part of this paper.

2. Materials and methods

Working voltage of the PV cell/system is first perturbed with an increase in PO calculation and then, the subsequent change of power is estimated and stored as a relative incentive in an algorithm [1].

If a positive change occurs in power, perturbation continues until a working point of the PV panel closer or equivalent to the MPP. On the other hand, negative change in power (diminishing control) after perturbations means that the operating point of the system is constantly getting away from the MPP. In this case, the direction of perturbation should be switched to draw the working point closer to the MPP. When the working point approaches the MPP, perturbation becomes positive again and, in this state, oscillations of the operating point begin around the MPP [21].

Perturbation is performed by changing the duty ratio, i.e., conduction time to total switching period, of DC-DC buck or boost converter. In PO calculation, duty cycle of the DC-DC buck converter is set as per the need. Thus, to transfer maximum power to battery/load from the source, source impedance of the battery/load and solar PV system is modified by adjusting duty cycle of the DC-DC converter [22].

The conventional PO and some of its variants used in the following comparison are discussed in Section 2.1.

2.1. Some PO methods

The conventional PO method has been compared with the modified PO [8], improved PO [23,24], and advanced PO [2] algorithms by the researchers for the battery and load cases. A brief review of these algorithms is given in the following.

2.1.1. Conventional PO method

Although conventional PO is a famous strategy, it has some downsides. Oscillations around the MPP and mediocre following velocity in quickly changing climate conditions are two downsides [25], which result in large power losses. Some strategies have

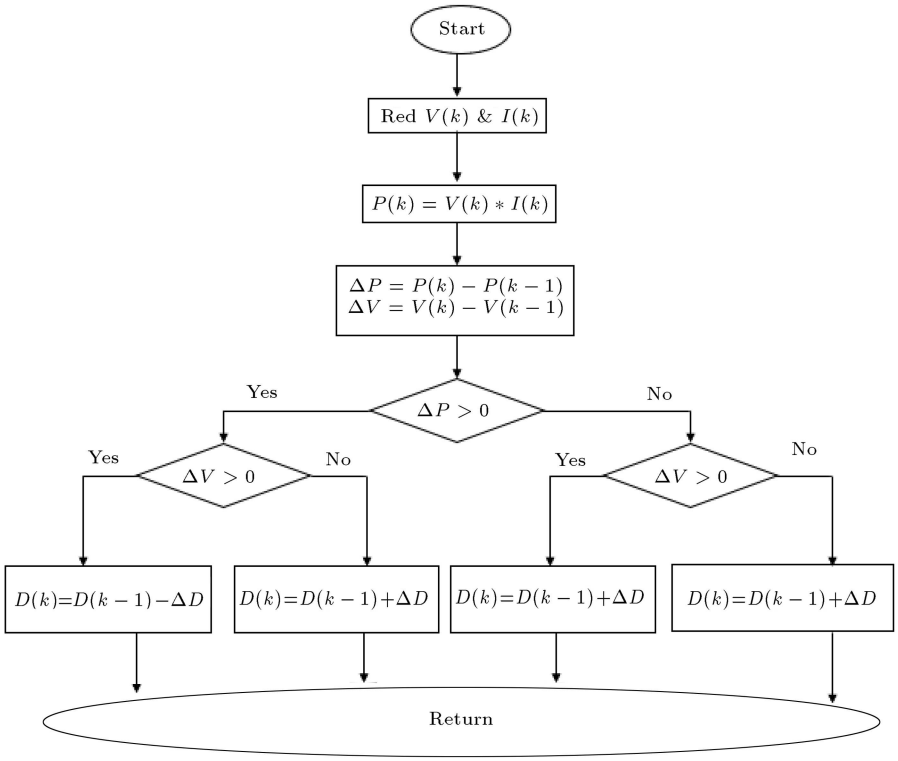

Figure 3. Flowchart of conventional PO method.

been suggested by Beydaghi et al. [25] and Santos and Galhardo [26] to tackle these issues. Abdelsalam et al. [27], by utilizing variable advance size, enhanced the conventional PO algorithm and could overcome the problems of slow tracking speed and oscillations around the MPP only to some extent. Flowchart of the conventional PO method is shown in Figure 3.

2.1.2. Modified PO method

An enhancement of the conventional PO method, namely modified PO, was suggested by Salas et al. [8]. Simplicity and high convergence speed were claimed to be the benefits of the modified PO method for MPPT applications. By utilizing different operating inputs in the calculations, it was demonstrated that the MPP was followed even in the cases of sudden change in illumination and load/battery level [8].

The modified PO MPPT calculation begins with calculating energy at the pre-set value of 100% for the duty cycle. Then, it estimates the real PV voltage, $V(k)$, and PV current, $I(k)$. At the next step, PV power, $P(k)$, is immediately estimated. Perturbation step size and duty ratio of the buck converter determine the error between $P(k)$ and $P(k-1)$. Then, the Metal-Oxide-Semiconductor Field-Effect Transistor (MOSFET) of the DC-DC buck converter is determined by the output of the MPPT controller for $P(k)$ to track the maximum power [6]. The flowchart of the modified PO method is shown in Figure 4.

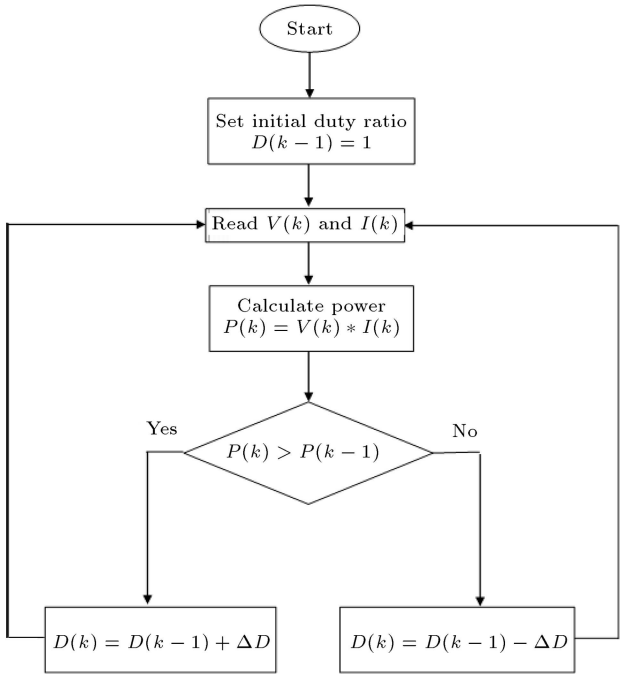

Figure 4. Flowchart of modified PO method.

2.1.3. Improved PO method

The conventional PO algorithm tracks the MPP with some oscillations around it and is favoured because of its basic structure. However, its MPPT calculations are valid only to the extent that changes in daylight radiation are consistent or changing is gradual [23,24].

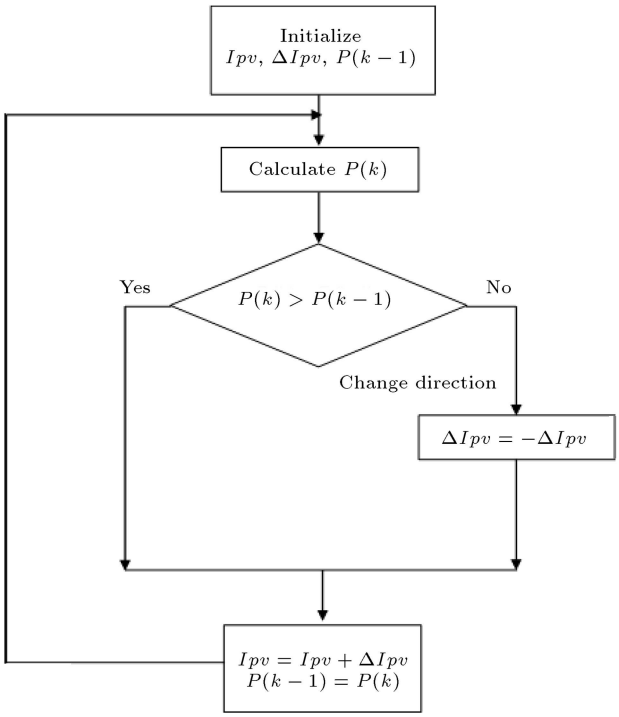

Figure 5. Flowchart of improved PO method.

This issue can be tackled to shorten the perturbation step; however, the tracking speed will be lower. To overcome the problems with the conventional PO, a new improvement [23,24] has been suggested, here referred to as improved PO method. The improved PO calculations are preferable in quickly changing climate conditions, where the usual PO calculations generally lead to considerable gaps between the working point of the system and the MPP. The flowchart of the improved PO method is shown in Figure 5.

2.1.4. A new PO variant (advanced PO method

Although variable advance size system utilized as a part of PO calculations makes quick reaction possible in following the MPP, the fundamental issue of oscillations of the operating point around MPP remains unresolved [2]. Awan et al. [2] utilized the "decline and fix" strategy to resolve this issue by changing PO calculation. The values of both variables of voltage and current are estimated to be used by the tracker in the advanced PO method [2]. The estimated voltage and current enable the tracker to identify whether the change of power is because of perturbation or due to variation in climate conditions (brightening or irradiance). The "decrease and fix" technique was replaced by the "decline and fix" technique by Awan et al. [2]. The flowchart of the advanced PO method is shown in Figure 6.

3. Results and discussion

To test the performance of the conventional PO and the enhancements discussed in Section 2, MATLAB Simulink was used to set up the circuit simulation diagrams as well as to obtain the rest of the results. The circuit diagrams used in the simulation for the cases of battery and load are shown in Figures 7 and 8, respectively, at the irradiance of 1000 W/m^2 and the temperature of 25°C. Other irradiance and temperature values were also used in the experiments, but they are not provided for the sake of brevity. The combinations of irradiances in the range of 0:250:1000 (W/m^2) with the temperatures ranging within 0:25:50 (°C) were considered in the simulations. Figure 9 shows the I-V and P-V curves for our experiments at the irradiances of 250 W/m^2 and 1000 W/m^2. Figure 10 shows the I-V and P-V characteristics at different temperature levels. In the load case, we used the resistor loads of 2.8 Ω, 5 Ω, 10 Ω, and 100 Ω.

The results for the conventional PO method with battery at an irradiance of 1000 W/m^2 and temperature of 25°C are shown in Figure 11. The voltage, current, and power curves versus time instants are shown. It can be seen that the conventional PO method successfully tracks the MPP and achieves the expected power level of 51 W. However, after the MPP, oscillations are observed, which are periodic in nature with constant amplitude around the MPP. The tracking speed is 0.027 s. Similarly, for the case of 2.8 Ω load, as evident in Figure 12, the voltage reaches near the MPP in a certain time and then, starts to oscillate around the MPP, causing constant-amplitude periodic oscillations at the power levels near MPP. Figure 12 shows that the expected power level has been achieved in the load case of 2.8 Ω and post MPP oscillations are the only concern with this method. Tables 1 and 2 summarize the input and output characteristics of the simulations with conventional PO method for all the cases of loads, namely 2.8 Ω, 5 Ω, 10 Ω, and 100 Ω, and at all values of irradiance and temperature.

Figures 13 and 14 demonstrate the performance of the modified PO method for the cases of battery and 2.8 Ω load at irradiance of 1000 W/m^2 and temperature of 25°C, respectively. It is clear in the figure that the modified PO method achieves the expected power level of 51 W faster than the conventional PO with an improved tracking speed of 0.002 s. Also, like the conventional PO, the modified PO suffers from post MPP oscillations. The oscillations are periodic with constant amplitude. In Figures 11 and 13, it is evident that the modified PO is superior to the conventional PO under similar conditions. On the other hand, for the case of 2.8 Ω load, the current, voltage, and power curves obtained by the modified PO method are shown in Figure 14. Also, for a more comprehensive understanding, the case for different loads, irradiances, and temperatures is presented in Tables 3 and 4. As seen in Figure 14, the modified PO method tracks the

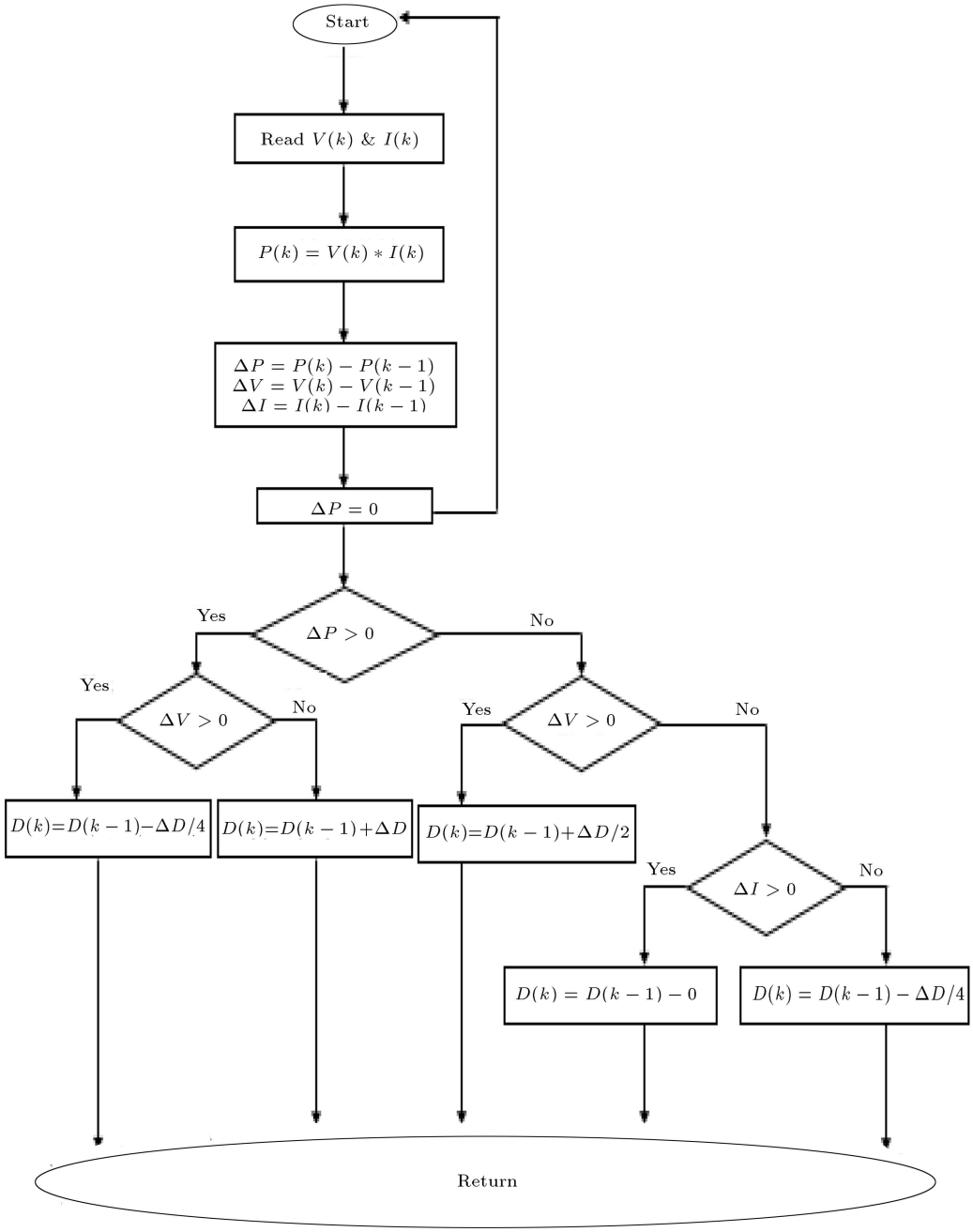

Figure 6. Flowchart of advanced PO method.

maximum power of 41 W, which is lower than the true/expected maximum power level. While tracking speed is very low and the achieved power level is lower, the modified PO method also exhibits oscillations around the obtained MPP. Moreover, the modified PO method does not yield successful simulations for the case of 10 Ω load with irradiance and temperatures pairs of (750, 25), (1000, 25), (1000, 50), and (1000, 0), as demonstrated in Tables 3 and 4.

The simulation results of the improved PO method for the cases of battery and load are not encouraging. In the cases of battery (Figure 15) and 2.8 Ω load (Figure 16), the expected maximum power level is not achieved. The obtained power levels by improved PO method are 37 W for battery and 27 W for 2.8 Ω load. It is interesting to note that the improved PO method does not exhibit any post MPP oscillations, while the achieved power level is much lower than expected, which can be considered as the main disadvantage of this method. The summary of input and output parameters for different loads, irradiances, and temperatures in the improved PO method for tracking the MPP is given in Tables 5 and 6. The cases for which the improved PO method

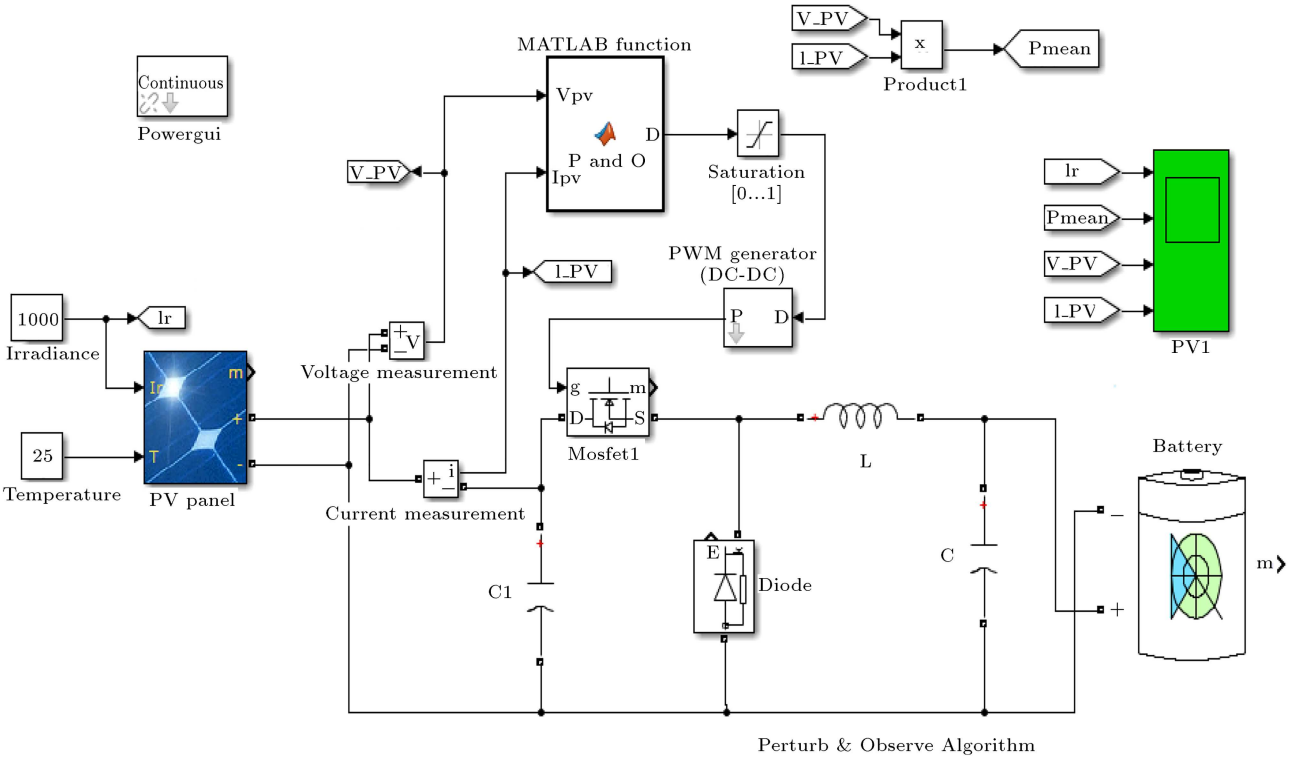

Figure 7. Simulation circuit diagram with battery.

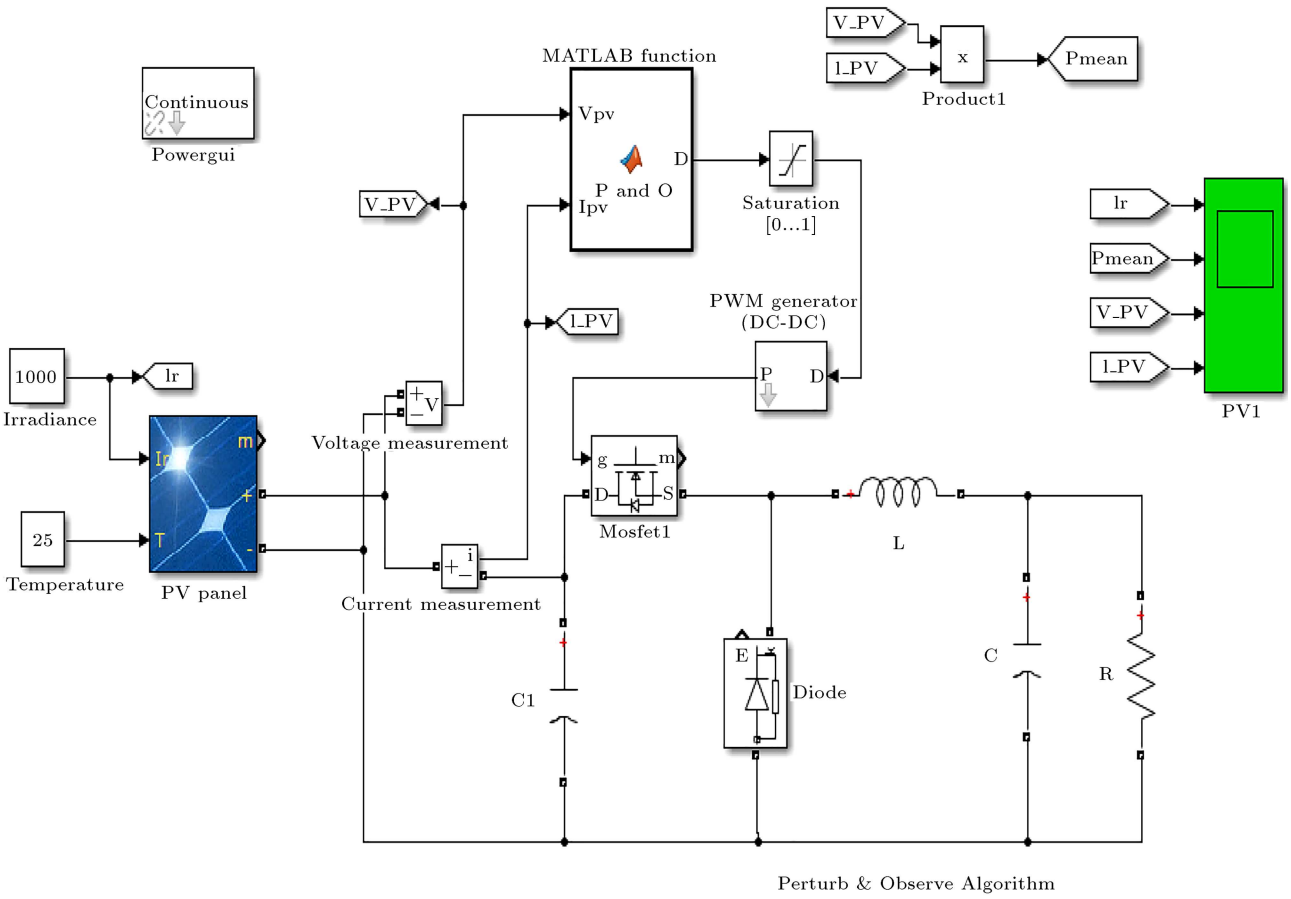

Figure 8. Simulation circuit diagram with load.

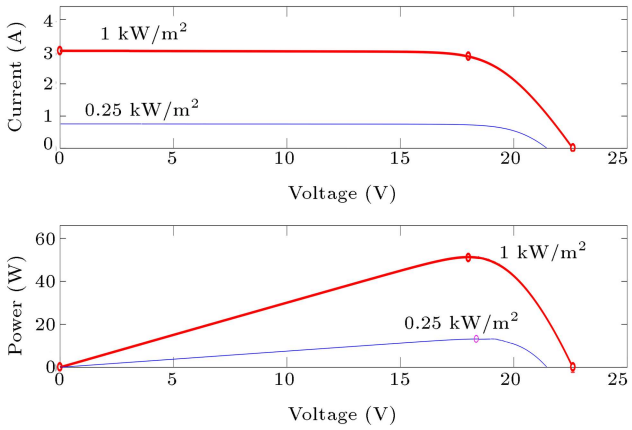

Figure 9. $I-V$ and $P-V$ curves for varying irradiance.

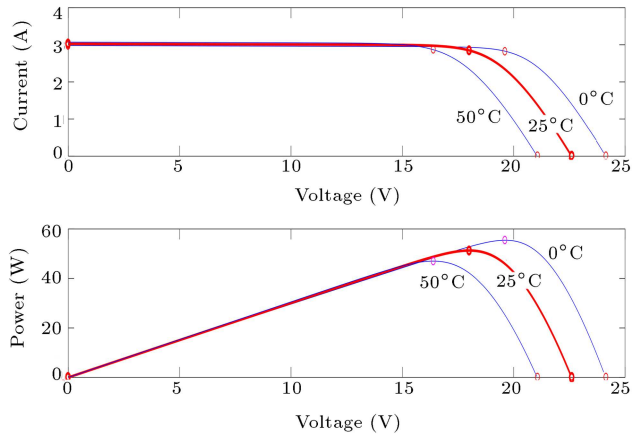

Figure 10. $I-V$ and $P-V$ curves for varying temperature.

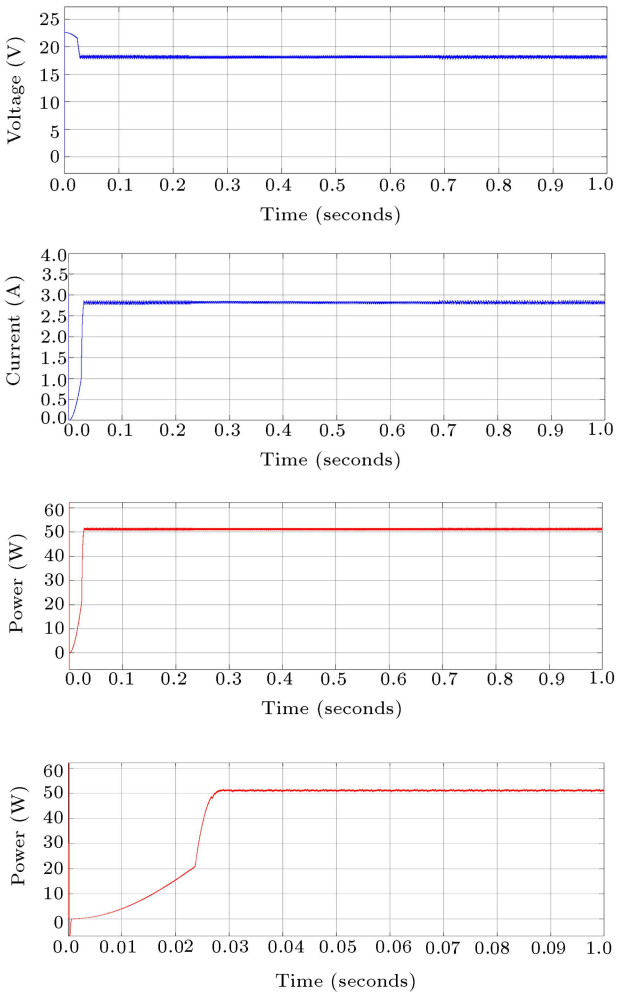

Figure 11. Results for the conventional PO method with battery.

does not conduct successful simulations are those with 1000 W/m^2, 25°C, and 10 Ω load and most of the combinations with 100 Ω load.

Figures 17 and 18 show the results of the advanced PO method for the cases of battery and 2.8 Ω load, respectively. The advanced PO method produces successful simulation results at all different loads, irradiances, and temperatures, as shown in Tables 7 and 8. Comparing the advanced PO method with the conventional PO method at standard test condition and voltage of PV panels, it is observed that in the advanced method, voltage reaches a level almost equal to the MPP very quickly and then, starts to oscillate. However, after some oscillations, which become smaller

Table 1. Input performance of the conventional PO method with different loads.

PV (W/m^2)	Temp (°C)	Load resistor = 2.8 Ω			Load resistor = 5 Ω			Load resistor = 10 Ω			Load resistor = 100 Ω		
		Voltage at input (V)	Current at input (A)	Power at input (W)	Voltage at input (V)	Current at input (A)	Power at input (W)	Voltage at input (V)	Current at input (A)	Power at input (W)	Voltage at input (V)	Current at input (A)	Power at input (W)
0	0	0	0	0	0	0	0	0	0	0	0	0	0
0	25	0	0	0	0	0	0	0	0	0	0	0	0
250	25	18.46	0.7113	13.13	18.51	0.7102	13.14	18.51	0.7116	13.17	21.04	0.2102	4.421
500	25	18.6	1.409	26.2	18.54	1.422	26.37	18.88	1.376	25.99	21.74	0.2172	4.722
750	25	18.63	2.094	39.02	18.63	2.074	38.63	19.36	1.917	37.11	22.1	0.2365	5.227
1000	25	18.34	2.784	51.05	18.26	2.792	50.99	20.21	2	40.42	22.37	0.2235	4.999
1000	50	16.61	2.823	46.89	16.8	2.782	46.72	18.82	1.864	35.08	20.84	0.2082	4.337
1000	0	19.97	2.782	55.54	19.88	2.781	55.3	21.57	2.135	46.06	23.89	0.2386	5.701

Table 2. Input-output performance of the conventional PO method with different loads.

PV (W/m^2)	Temp (°C)	Load resistor = 2.8 Ω			Load resistor = 5 Ω			Load resistor = 10 Ω			Load resistor = 100 Ω		
		Voltage at input (V)	Voltage at output (V)	Current at output (A)	Voltage at input (V)	Voltage at output (V)	Current at output (A)	Voltage at input (V)	Voltage at output (V)	Current at output (A)	Voltage at input (V)	Voltage at output (V)	Current at output (A)
0	0	0	0	0	0	0	0	0	0	0	0	0	0
0	25	0	0	0	0	0	0	0	0	0	0	0	0
250	25	18.46	5.745	2.052	18.51	7.834	1.567	18.51	11.09	1.109	21.04	21.02	0.2102
500	25	18.6	8.255	2.948	18.54	11.23	2.246	18.88	16	1.6	21.74	21.72	0.2172
750	25	18.63	10.18	3.637	18.63	13.73	2.746	19.36	19.17	1.917	22.1	22.09	0.2209
1000	25	18.34	11.64	4.158	18.26	15.79	3.157	20.2	20	2	22.37	22.35	0.2235
1000	50	16.61	11.18	3.992	16.8	15.13	3.026	18.82	18.64	1.864	20.84	20.82	0.2082
1000	0	19.97	12.13	4.332	19.88	16.46	3.293	21.57	21.35	2.135	23.89	23.86	0.2386

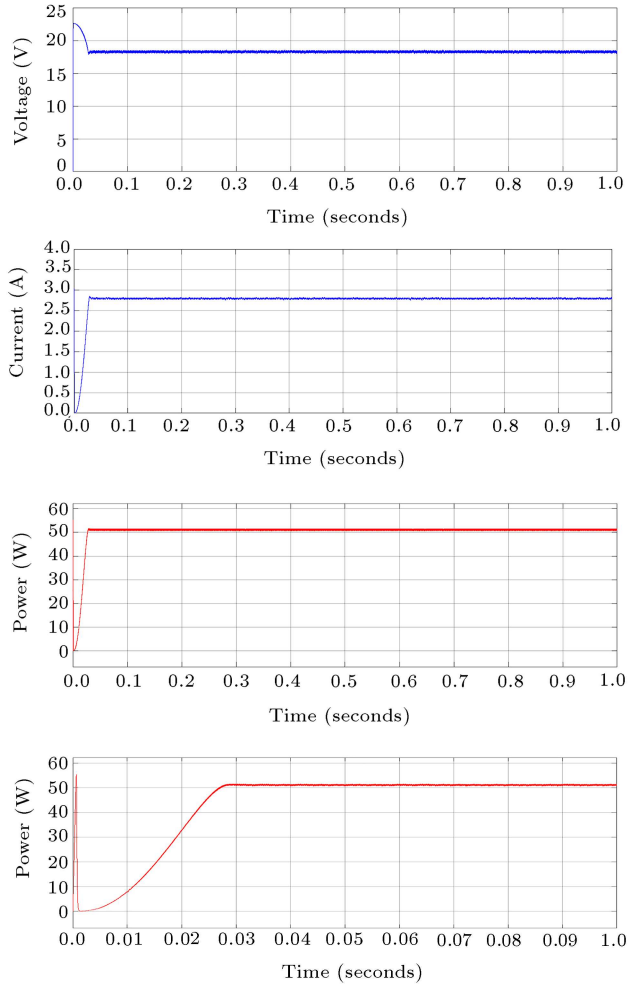

Figure 12. Results for the conventional PO method with the load of 2.8 Ω.

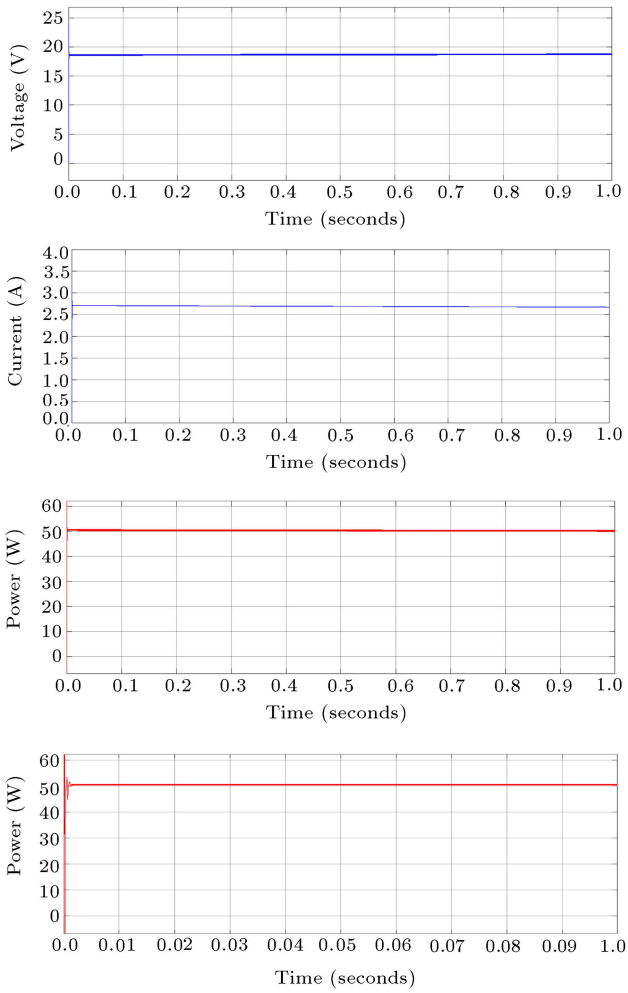

Figure 13. Results for the modified PO method with battery.

and smaller, it attains the MPP. The oscillations have decreasing behaviour as time advances and the method achieves the expected maximum power level of 51 W in both cases of battery and loads. Tracking speed for the case of battery is 0.027 s, i.e., the advanced method is slightly quicker than the conventional method, whereas for the case of 2.8 Ω load, the speeds of both methods are same, i.e., 0.027 s. The margin of improvement of the advanced PO method is quite significant for battery and load cases, especially with regard to the decreasing oscillations. As shown in Figures 17 and 18 and Tables 7 and 8, it is an efficient enhancement

Table 3. Input performance of the modified PO method with different loads.

PV (W/m^2)	Temp (°C)	Load resistor = 2.8 Ω			Load resistor = 5 Ω			Load resistor = 10 Ω			Load resistor = 100 Ω		
		Voltage at input (V)	Current at input (A)	Power at input (W)	Voltage at input (V)	Current at input (A)	Power at input (W)	Voltage at input (V)	Current at input (A)	Power at input (W)	Voltage at input (V)	Current at input (A)	Power at input (W)
0	0	0	0	0	0	0	0	0	0	0	0	0	0
0	25	0	0	0	0	0	0	0	0	0	0	0	0
250	25	2.193	0.7562	1.658	3.853	0.7555	2.911	7.615	0.7539	5.741	21.06	0.2016	4.247
500	25	4.739	1.51	6.613	7.687	1.507	11.59	15.15	1.5	22.72	21.64	0.2864	6.198
750	25	6.559	2.262	14.83	11.5	2.255	25.94	NA	NA	NA	22.03	0.2907	6.405
1000	25	8.732	3.011	26.29	15.27	2.994	45.72	NA	NA	NA	22.28	0.3071	6.842
1000	50	8.866	3.057	27.11	15.26	2.992	45.65	NA	NA	NA	20.76	0.2825	5.863
1000	0	8.597	2.965	25.49	15.06	2.953	44.49	NA	NA	NA	23.8	0.3295	7.842

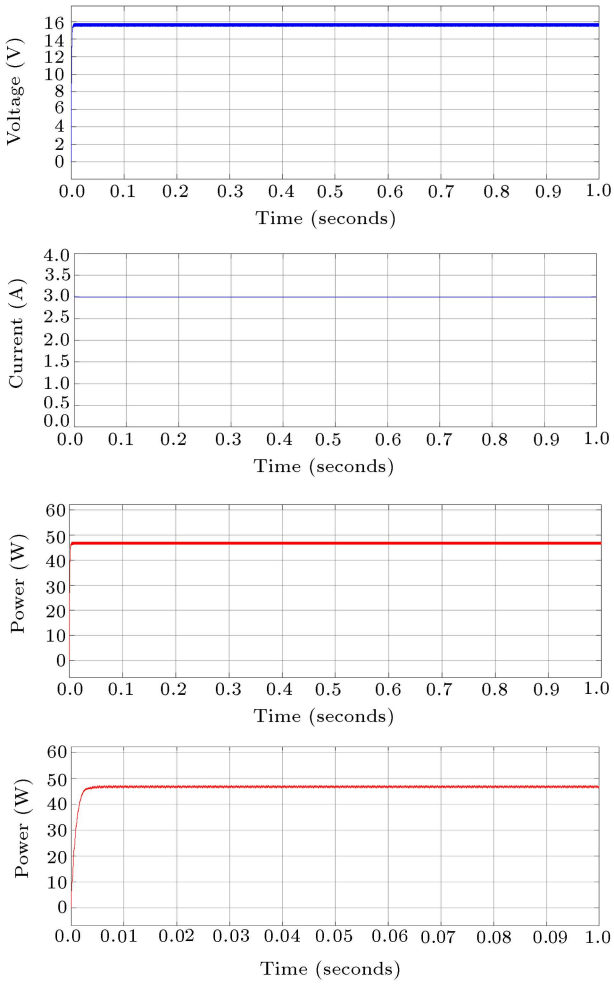

Figure 14. Results for the modified PO method with the load of 2.8 Ω.

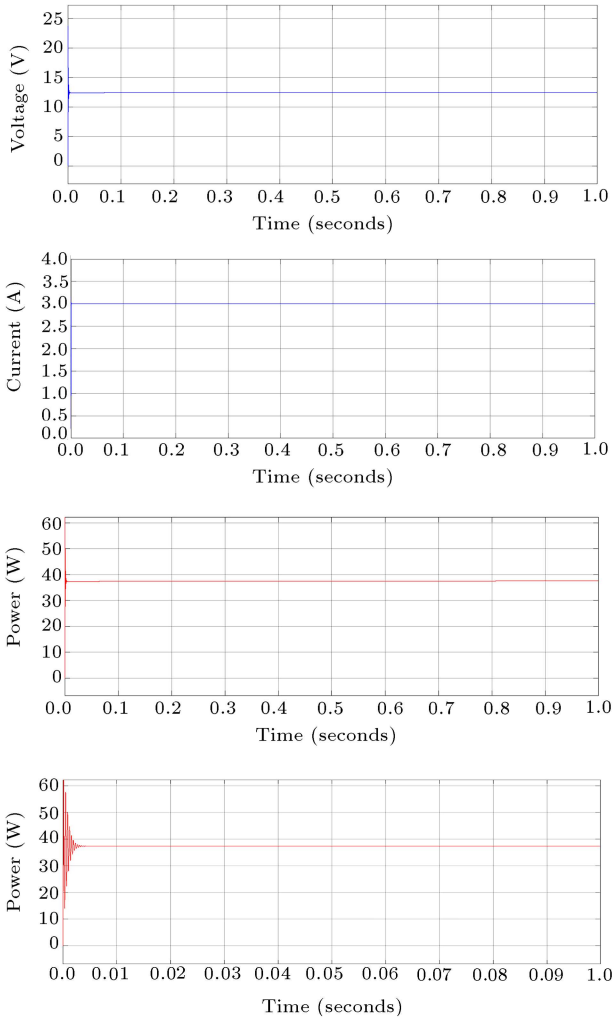

Figure 15. Results for the improved PO method with battery.

of the conventional PO method with no or decreasing oscillations around the MPP.

Tables 9 and 10 highlight the observed properties of all PO variants used in this study on the basis of the simulations performed. For the case of battery, tracking speed of the advanced PO method is the quickest among all methods. The power level is achieved by all methods, except for the improved PO method in the case of battery. In Table 9, it appears that all the three successful methods have oscillations, but the oscillations in the advanced PO method decrease

Table 4. Input-output performance of the modified PO method with different loads.

PV (W/m^2)	Temp (°C)	Load resistor = 2.8 Ω			Load resistor = 5 Ω			Load resistor = 10 Ω			Load resistor = 100 Ω		
		Voltage at input (V)	Voltage at output (V)	Current at output (A)	Voltage at input (V)	Voltage at output (V)	Current at output (A)	Voltage at input (V)	Voltage at output (V)	Current at output (A)	Voltage at input (V)	Voltage at output (V)	Current at output (A)
0	0	0	0	0	0	0	0	0	0	0	0	0	0
0	25	0	0	0	0	0	0	0	0	0	0	0	0
250	25	2.193	2.117	0.7562	3.853	3.777	0.7555	7.615	7.539	0.7539	21.01	20.87	0.2087
500	25	4.739	4.228	1.51	7.687	7.537	1.507	15.15	15	1.5	21.64	21.54	0.2154
750	25	6.559	6.333	2.262	11.5	11.28	2.255	NA	NA	NA	22.03	21.91	0.2191
1000	25	8.732	8.431	3.011	15.27	14.97	2.994	NA	NA	NA	22.28	22.19	0.2219
1000	50	8.866	8.56	3.057	15.26	14.96	2.992	NA	NA	NA	20.76	20.66	0.2066
1000	0	8.597	8.301	2.965	15.06	14.77	2.953	NA	NA	NA	23.8	23.79	0.2379

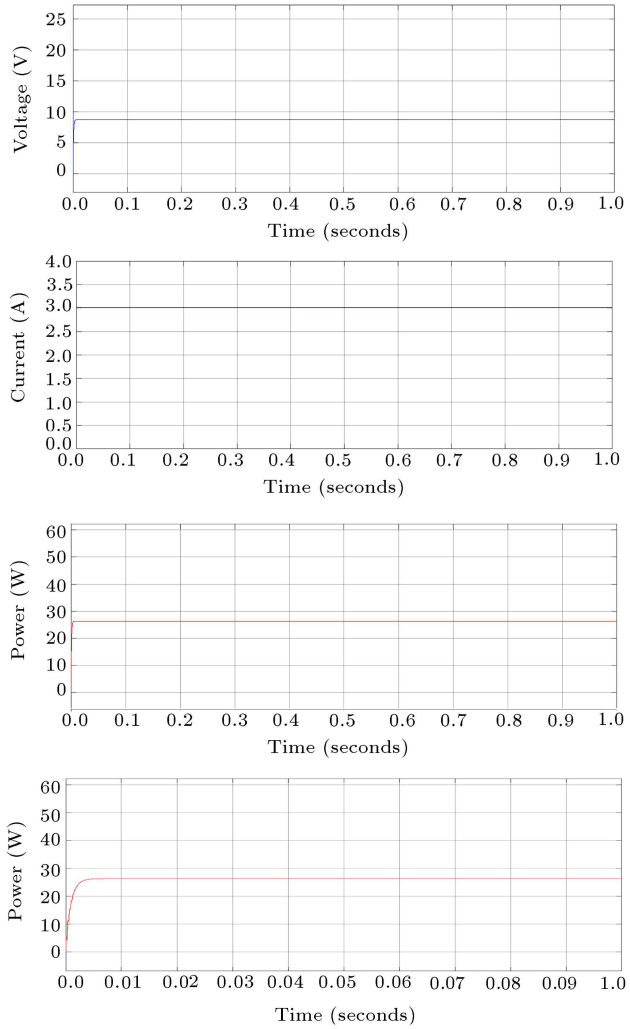

Figure 16. Results for the improved PO method with the load of 2.8 Ω.

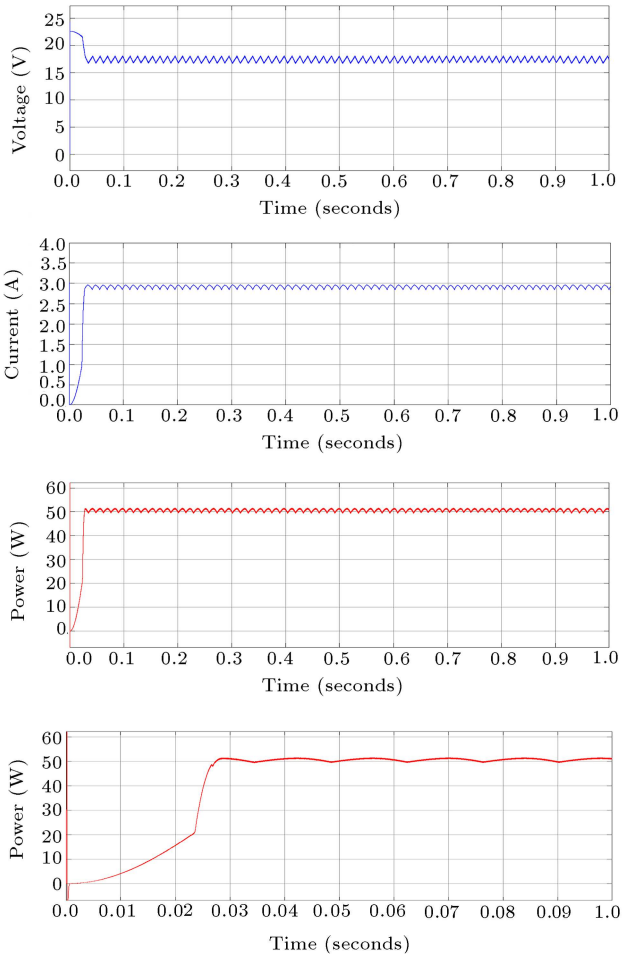

Figure 17. Results for the advanced PO method with battery.

gradually. For the case of 2.8 Ω load, as seen in Table 10, only the conventional and advanced PO methods achieve the expected maximum power level with the same tracking speed. However, the advanced PO is superiors because of decreasing oscillations. These results are in line with the simulations presented by Awan et al. [2]. In Table 11, the key characteristics of all the variants of the PO method considered in this work are summarized. All the methods lead to the control duty cycle and use both current and voltage

Table 5. Input performance of the improved PO method with different loads.

PV (W/m^2)	Temp (°C)	Load resistor = 2.8 Ω			Load resistor = 5 Ω			Load resistor = 10 Ω			Load resistor = 100 Ω		
		Voltage at input (V)	Current at input (A)	Power at input (W)	Voltage at input (V)	Current at input (A)	Power at input (W)	Voltage at input (V)	Current at input (A)	Power at input (W)	Voltage at input (V)	Current at input (A)	Power at input (W)
0	0	0	0	0	0	0	0	0	0	0	0	0	0
0	25	0	0	0	0	0	0	0	0	0	0	0	0
250	25	4.051	0.7554	3.06	6.93	0.7542	5.226	13.56	0.7513	10.19	NA	NA	NA
500	25	4.379	1.51	6.613	7.687	1.507	11.59	15.15	1.5	22.72	NA	NA	NA
750	25	6.559	2.262	14.83	11.5	2.255	25.94	19.36	1.917	37.11	NA	NA	NA
1000	25	8.732	3.011	26.29	15.27	2.994	45.72	NA	NA	NA	NA	NA	NA
1000	50	8.866	3.057	27.11	15.26	2.992	45.65	18.82	1.864	35.08	NA	NA	NA
1000	0	8.597	2.965	25.49	15.06	2.953	44.49	21.57	2.135	46.06	NA	NA	NA

Table 6. Input-output performance of the improved PO method with different loads.

PV (W/m^2)	Temp (°C)	Load resistor = 2.8 Ω			Load resistor = 5 Ω			Load resistor = 10 Ω			Load resistor = 100 Ω		
		Voltage at input (V)	Voltage at output (V)	Current at output (A)	Voltage at input (V)	Voltage at output (V)	Current at output (A)	Voltage at input (V)	Voltage at output (V)	Current at output (A)	Voltage at input (V)	Voltage at output (V)	Current at output (A)
0	0	0	0	0	0	0	0	0	0	0	0	0	0
0	25	0	0	0	0	0	0	0	0	0	0	0	0
250	25	4.051	2.789	0.9961	6.93	4.979	0.9958	13.56	9.917	0.9917	NA	NA	NA
500	25	4.379	4.228	1.51	7.687	7.537	1.507	15.15	15	1.5	NA	NA	NA
750	25	6.559	6.333	2.262	11.5	11.28	2.255	19.36	19.17	1.917	NA	NA	NA
1000	25	8.732	8.431	3.011	15.27	14.97	2.994	NA	NA	NA	NA	NA	NA
1000	50	8.866	8.56	3.057	15.26	14.96	2.992	18.82	18.64	1.864	NA	NA	NA
1000	0	8.597	8.301	2.965	15.06	14.77	2.953	21.57	21.35	2.135	NA	NA	NA

Table 7. Input performance of the advanced PO method with different loads.

PV (W/m^2)	Temp (°C)	Load resistor = 2.8 Ω			Load resistor = 5 Ω			Load resistor = 10 Ω			Load resistor = 100 Ω		
		Voltage at input (V)	Current at input (A)	Power at input (W)	Voltage at input (V)	Current at input (A)	Power at input (W)	Voltage at input (V)	Current at input (A)	Power at input (W)	Voltage at input (V)	Current at input (A)	Power at input (W)
0	0	0	0	0	0	0	0	0	0	0	0	0	0
0	25	0	0	0	0	0	0	0	0	0	0	0	0
250	25	17.44	0.7396	12.9	18.05	0.7255	13.1	18.1	0.7257	13.14	21.0 4	0.2102	4.421
500	25	17.88	1.466	26.2	18.17	1.445	26.25	18.11	1.452	26.29	21.74	0.2172	4.722
750	25	17.93	2.165	38.82	18.17	2.145	39.98	19.36	1.917	37.11	22.11	0.2209	4.885
1000	25	17.66	2.897	51.18	17.64	2.895	51.07	20.21	2	40.42	22.37	0.2235	4.999
1000	50	16.18	2.913	47.11	15.61	2.966	46.31	18.82	1.864	35.08	20.84	0.2082	4.337
1000	0	19.28	2.856	55.07	19.26	2.864	55.18	21.57	2.135	46.06	23.89	0.2386	5.701

for MPPT in the search for the MPP, except for the improved PO method, which uses only information of currents to track the MPP. The advanced PO is considered as a moderating MPPT method as it achieves the true power and its oscillations, if any, are decreasing in nature. The conventional and modified PO are moderate tracking methods for the battery cases, whereas the latter is not reliable enough in the cases of loads. The improved PO method is slower and it does not achieve the expected power level.

Table 12 summarises the outcomes of an experimental investigation by real implementation of a similar system to look into validity and reliability of the simulation results. In the experiments, the PV was 750 W/m^2 at the temperature was 25°C. The figures for the real-time implementation are not exactly the

Table 8. Input-output performance of the advanced PO method with different loads.

PV (W/m^2)	Temp (°C)	Load resistor = 2.8 Ω			Load resistor = 5 Ω			Load resistor = 10 Ω			Load resistor = 100 Ω		
		Voltage at input (V)	Voltage at output (V)	Current at output (A)	Voltage at input (V)	Voltage at output (V)	Current at output (A)	Voltage at input (V)	Voltage at output (V)	Current at output (A)	Voltage at input (V)	Voltage at output (V)	Current at output (A)
0	0	0	0	0	0	0	0	0	0	0	0	0	0
0	25	0	0	0	0	0	0	0	0	0	0	0	0
250	25	17.44	5.673	2.026	18.05	7.827	1.565	18.1	1.122	11.22	21.04	21.02	0.2102
500	25	17.88	8.246	2.945	18.18	11.22	2.245	18.11	16.09	1.609	21.74	21.72	0.2172
750	25	17.93	10.17	3.631	18.17	13.72	2.745	19.36	19.17	1.917	22.11	22.09	0.2209
1000	25	17.66	11.68	4.17	17.64	15.76	3.151	20.2	20	2	22.37	22.35	0.2235
1000	50	16.18	11.19	3.996	15.61	15.09	3.019	18.82	18.64	1.864	20.84	20.82	0.2082
1000	0	19.28	12.13	4.331	19.26	16.39	3.278	21.57	21.35	2.135	23.89	23.86	0.2386

Table 9. Performance indicators for different PO variants with battery.

Serial number	PO method	Tracking speed	Power level achieved	Post oscillations	Power obtained
1	Conventional	0.028 seconds	Yes	Yes (constant amplitude, periodic)	51 W
2	Modified	0.002 seconds	Yes	Yes (constant amplitude, periodic)	51 W
3	Improved	0.004 seconds	No	No	37 W
4	Advanced	0.027 seconds	Yes	No or decreasing oscillations	51 W

Table 10. Performance indicators for different PO variants with 2.8 Ω load.

Serial number	PO method	Tracking speed	Power level achieved	Post oscillations	Power obtained
1	Conventional	0.027 seconds	Yes	Yes (constant amplitude, periodic)	51 W
2	Modified	0.004 seconds	No	Yes (constant amplitude, periodic)	46 W
3	Improved	0.007 seconds	No	No	27 W
4	Advanced	0.027 seconds	Yes	No or decreasing oscillations	51 W

Table 11. Summary of the characteristics of PO variants.

Serial number	PO method	Input required	Output	Total possible conditions	Tracking speed
1	Conventional	Vpv, Ipv	Controlled duty cycle	4	Moderate
2	Modified	Vpv, Ipv	Controlled duty cycle	2	Moderate
3	Improved	Ipv	Controlled duty cycle	2	Slower
4	Advanced	Vpv, Ipv	Controlled duty cycle	5	Faster

same as the simulation results due to changing weather conditions, stochastic nature of the environmental effects, shading conditions, etc. While the experimental results in the figure are expected to be lower than the simulation results, they can help in understanding the reliability and efficiency of the approximations by computing algorithms. For a series of results recorded from 9:00 AM to 4:00 PM every hour, Table 12 shows that the maximum power levels are 38.7 W at 12:00 PM and 39.6 W at 1:00 PM, which are naturally the best conditions for the working of solar PV systems. The simulation results for the same conditions with the conventional, modified, improved, and advanced PO methods in Tables 1-8 can be compared with the experimental results in Table 12. The comparison is also extended in Figure 19 only for the cases of 2.8 Ω, 5 Ω, and 10 Ω for the sake of brevity. The new advanced PO variant shows an edge over the other methods. Also, the efficiency of the conventional PO algorithm is demonstrated in the figure. It shows the

Table 12. Experimental results for 750 W/m^2 at 25°C from 9:00 AM to 04:00 PM.

Serial number	Time of reading	V_{in} (V)	I_{in} (A)	V_{out} (V)	Power (W)
1	09:00 AM	17.2	2.10	12.57	36.12
2	10:00 AM	17.0	2.10	12.51	35.70
3	11:00 AM	17.4	2.05	12.51	35.70
4	12:00 PM	18.0	2.15	12.45	**38.70 ($P_{\max}$)**
5	01:00 PM	18.31	2.16	12.60	**39.60 ($P_{\max}$)**
6	02:00 PM	17.8	2.14	12.49	38.20
7	03:00 PM	17.9	2.11	12.47	37.93
8	04:00 PM	17.23	2.19	12.53	37.80

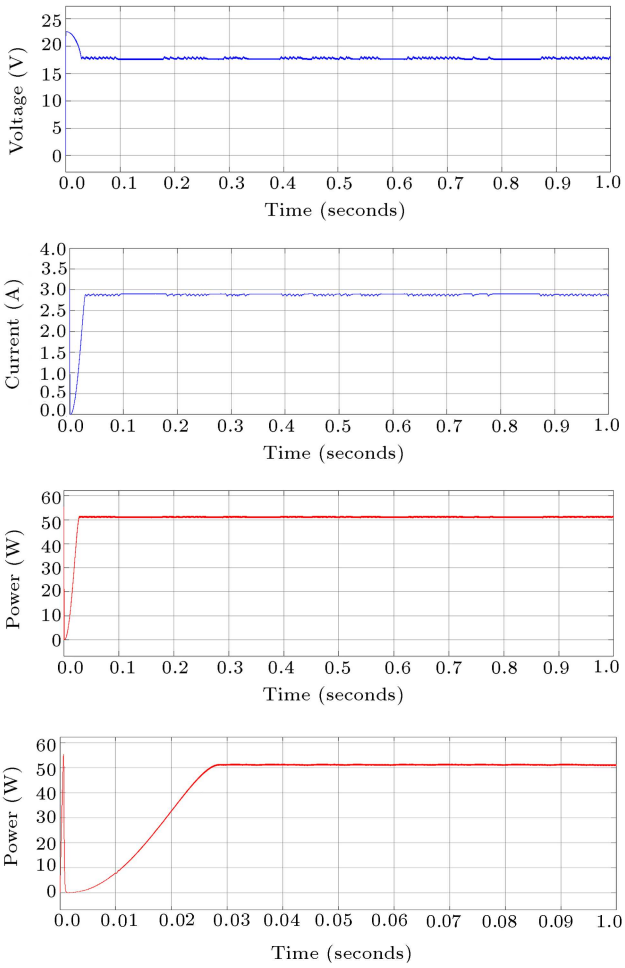

Figure 18. Results for the advanced PO method with the load of 2.8 Ω.

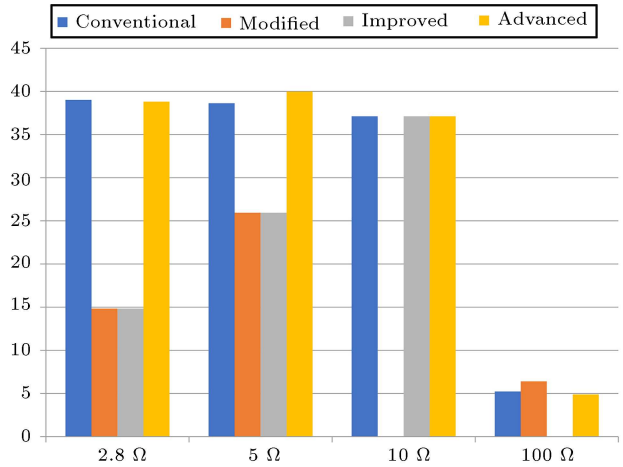

Figure 19. Validation of the simulated PO variants against the experimental results.

over-approximations of the modified and improved PO methods, proving that they are not applicable to the considered cases. The new advanced PO method can be used in the future for fast and reliable tracking of MPP in the PV solar systems.

4. Conclusion

A comparative study of some existing variants of the PO method for MPPT in PV solar panels was conducted. The performance of the conventional, modified, improved, and advanced PO methods was tested for the cases of battery and different loads. Three major issues with PV panels, namely oscillations, slow tracking speed, and reactions in changing climate conditions, were addressed through simulations to investigate the efficiency of the considered PO methods. The "decline and fix" strategy in the advanced PO method established it superiority over other methods in the overall comparison by resolving the oscillations at the MPP operating point, which is a major challenge to the productivity of PV systems.

Nomenclature

PV	Photovoltaic
MPP	Maximum Power Point
MPPT	Maximum Power Point Tracking
PO	Perturb and Observe
V_{mpp}	Voltage level at MPP
P_{mpp}	Power level at MPP
$I-V$	Current voltage
$P-V$	Power voltage

HC	Hill Climbing
INC	Incremental conductance
FL	Fuzzy Logic
PS	Particle Swam
DC	Direct Current
MOSFET	Metal-Oxide-Semiconductor Field-Effect Transistor

References

1. Azab, M. "A new maximum power point tracking for photovoltaic systems", *WASET. ORG*, **34**, pp. 571-574 (2008).
2. Awan, M.M., Afzal, M., and Awan, F.G. "Improvement of maximum power point tracking perturb and observe algorithm for a standalone solar photovoltaic system", *Mehran University Research Journal of Engineering and Technology*, **36**(3), pp. 501-510 (2017).
3. Putri, R.I., Wibowo, S., and Rifa'I, M. "Maximum power point tracking for photovoltaic using incremental conductance method", *Energy Procedia*, **68**, pp. 22-30 (2015).
4. Babaa, S.E., Armstrong, M., and Pickert, W. "Overview of maximum power point tracking control methods for PV systems", *Journal of Power and Energy Engineering*, **2**(8), p. 59 (2014).
5. Rezk, H. and Eltamaly, A.M. "A comprehensive comparison of different MPPT techniques for photovoltaic systems", *Solar Energy*, **112**, pp. 1-11 (2015).
6. Bahrami, M., Gavagsaz-Ghoachani, R., Zandi, M., et al. "Hybrid maximum power point tracking algorithm with improved dynamic performance", *Renewable Energy*, **130**, pp. 982-991 (2019).
7. Chaieb, H. and Sakly, A. "A novel MPPT method for photovoltaic application under partial shaded conditions", *Solar Energy*, **159**, pp. 291-299 (2018).
8. Salas, V., Olias, E., Barrado, A., et al. "Review of the maximum power point tracking algorithms for standalone photovoltaic systems", *Solar Energy Materials and Solar Cells*, **90**(11), pp. 1555-1578 (2006).
9. Thenkani, A. and Kumar, N.S. "Design of optimum maximum power point tracking algorithm for solar panel", *International Conference on Computer, Communication and Electrical Technology (ICCCET), IEEE* (2011).
10. Abdel-Salam, M., El-Mohandes, M., and Goda, M. "An improved perturb-and-observe based MPPT method for PV systems under varying irradiation levels", *Solar Energy*, **171**, pp. 547-561 (2018).
11. Devi, V.K., Premkumar, K., Beevi, A.B., et al. "A modified perturb & observe MPPT technique to tackle steady state and rapidly varying atmospheric conditions", *Solar Energy*, **157**, pp. 419-426 (2017).
12. Alik, R. and Jusoh, A. "Modified perturb and observe (P&O) with checking algorithm under various solar irradiation", *Solar Energy*, **148**, pp. 128-139(2017).
13. Özçelik, M.A. and Yılmaz, A.S. "Effect of maximum power point tracking in photovoltaic systems and its improving and its application of wireless energy transmission", *Journal of Clean Energy Technologies*, **3**(6), pp. 441-416 (2015).
14. Soulatiantork, P. "Performance comparison of a two PV module experimental setup using a modified MPPT algorithm under real outdoor conditions", *Solar Energy*, **169**, pp. 401-410 (2018).
15. Alik, R. and Jusoh, A. "An enhanced P&O checking algorithm MPPT for high tracking efficiency of partially shaded PV module", *Solar Energy*, **163**, pp. 570-580 (2018).
16. Rajani, S.V. and Pandya, V.J. "Experimental verification of the rate of charge improvement using photovoltaic MPPT hardware for the battery and ultracapacitor storage devices", *Solar Energy*, **139**, pp. 142-148 (2016).
17. Tang, R., Wu, Z., and Fang, Y. "Configuration of marine photovoltaic system and its MPPT using model predictive control", *Solar Energy*, **158**, pp. 995-1005 (2017).
18. Shahid, H., Kamran, M., Mehmood, Z., et al. "Implementation of the novel temperature controller and incremental conductance MPPT algorithm for indoor photovoltaic system", *Solar Energy*, **163**, pp. 235-242 (2018).
19. Arsalan, M., Iftikhar, R., Ahmad, I., et al. "MPPT for photovoltaic system using nonlinear backstepping controller with integral action", *Solar Energy*, **170**, pp. 192-200 (2018).
20. El-Khatib, M.F., Shaaban, S., and El-Sebah, M.I. "A proposed advanced maximum power point tracking control for a photovoltaic-solar pump system", *Solar Energy*, **158**, pp. 321-331 (2017).
21. Gomathy, S., Saravanan, S., and Thangavel, S. "Design and implementation of maximum power point tracking (MPPT) algorithm for a standalone PV system", *International Journal of Scientific & Engineering Research*, **3**(3), pp. 1-7 (2012).
22. Swathy, A. and Archana, R. "Maximum power point tracking using modified incremental conductance for solar photovoltaic system", *Int. J. Eng. Innov. Technol.(IJEIT)*, **3**(2), pp. 333-337 (2013).
23. Esram, T. and Chapman, P.L. "Comparison of photovoltaic array maximum power point tracking techniques", *IEEE Transactions on Energy Conversion*, **22**(2), pp. 439-449 (2007).

24. Wanzeller, M.G., Alves, R.N.C., da Fonseca Neto, J.V., et al. "Current control loop for tracking of maximum Alves, power point supplied for photovoltaic array", *IEEE Transactions on Instrumentation and Measurement*, **53**(4), pp. 1304-1310 (2004).

25. Beydaghi, S., Vahidi, B., Ankouti, Y., et al. "Simulation of improved perturb and observe MPPT using Sepic converter", *Science International*, **27**(3) (2015).

26. Santos, T.J.A. and Galhardo, A. "A perturbation and observation routine used to control a power converter", *Sixth World Congress on Nature and Biologically Inspired Computing (NaBIC), IEEE* (2014).

27. Abdelsalam, A.K., Massoud, A.M., Ahmed, S., et al. "High-performance adaptive perturb and observe MPPT technique for photovoltaic-based microgrids", *IEEE Transactions on Power Electronics*, **26**(4), pp. 1010-1021 (2011).

Biographies

Veer Bhan received the BE (Electrical Engineering) from Mehran University of Engineering and Technology, Pakistan, in 2017. Currently, he is pursuing his ME (Electrical Power) in the same department. Besides, he is serving as Lecturer at the Department of Electrical Engineering, IBA University, Sukkur, Pakistan.

Ashfaque Ahmed Hashmani received the BE (Electrical Engineering) from Mehran University of Engineering and Technology, Pakistan; ME in Singapore; and PhD from University of Duisberg-Essen, Germany. Currently, he is a Professor and the Chairman in the Department of Electrical Engineering, Mehran University of Engineering and Technology. His fields of interest are power system stability and control, nonlinear control and applications, and robust control of power and energy systems.

Muhammad Mujtaba Shaikh is working as an Assistant Professor of Mathematics in the Department of Basic Sciences and Related Studies, Mehran University of Engineering and Technology, Jamshoro, Pakistan. He received PhD (Mathematics) from the Institute of Mathematics and Computer Science, University of Sindh, Jamshoro, Pakistan, in 2017. He was awarded gold and silver medals during his BS (Mathematics) studies in 2009. He is an active researcher having total impact factor of over 20, according to the reputed Journal Citations Reports by Thompson Reuters. He has profound knowledge of computational methods and statistical analysis, and has been involved in teaching and research in these fields using various tools including MATLAB, SPSS, CTSM-R, TORA, etc. His research fields include optimization, numerical integration, applied and computational mathematics, and mathematical problems in engineering. He is also an active member of Supply Chain and Operations Management (SCOM) research group at Mehran UET. Also, a number of research scholars are working under his supervision in BE, MS, ME, MPhil and PhD programs.